3D quantitative structure activity relationships with CoRSA. Comparative receptor surface analysis. Application to calcium channel agonists*

O. Ivanciuc,[1] T. Ivanciuc,[1] and D. Cabrol-Bass[2,*]

[1]*Department of Organic Chemistry, Faculty of Chemical Technology, University "Politehnica" of Bucharest, Oficiul 12 CP 243, 78100 Bucharest, Romania*

[2]*Groupe Chimiométrie et Modélisation. Laboratoire Arômes, Synthèses, Interactions, Université de Nice-Sophia Antipolis, Parc Valrose, 06108 Nice Cedex 2, France*

The *in vitro* or *in vivo* interaction between chemical compounds and their biological targets (transporters, receptors, ion channels, enzymes) can be efficiently predicted with the 3D QSAR models introduced in recent years. In this paper we describe CoRSA (comparative receptor surface analysis), a novel 3D QSAR algorithm that can be applied to compute structure-activity equations whenever the structure of the biological target is not known. Using the common steric and electrostatic features of the most active members of a series of compounds, CoRSA generates a virtual receptor model, represented as points on a surface complementary to the van der Waals surface of the set of compounds. The structural descriptors of the model are represented by the total interaction energies between each surface point of the virtual receptor and all atoms in a molecule. These descriptors are used in a partial least squares (PLS) data analysis to generate a structure-activity model. A highly significant CoRSA model was obtained for a set of compounds that act as calcium channel agonists for the guinea pig left atrium assay.

Introduction

The interaction with specific biological targets (enzymes, transporters, ion channels, or receptors) is responsible for the therapeutic action of a large number of drugs. In the past, drug discovery was mainly the result of chance discovery and massive screening of large corporate libraries of synthesized or naturally-occurring compounds. Nowadays, this time-consuming and expensive process uses various techniques of computer-aided ligand design [1,2]. This rational approach to the design of ligand-receptor interaction was made possible by the recent advances in various fields of computational chemistry, such as molecular graphics, molecular mechanics, quantum chemistry, molecular dynamics, library searching, prediction of physical, chemical, and biological properties. An important step in ligand design is to find a lead, a compound that binds to the target receptor. Leads can be generated using techniques of *de novo* ligand design or can be discovered by *in vitro* screening of large corporate libraries. We have to mention that the lead identification is only the beginning of a long and expensive process that eventually yields a commercial drug. A lead may have a low affinity for the target receptor, may be too unstable in solution, too toxic, too rapidly eliminated or metabolized, too difficult or expensive to synthesize in large quantities. Because the screening procedures generally give leads that are not suitable as commercial drugs, these compounds have to be optimized using various techniques of computer-aided ligand design. The availability of three-dimensional (3D) structural information of biological receptors and their complexes with various ligands can be extremely useful in suggesting ways to improve the affinity of the lead to the target. Because in many cases such detailed structural information is still unavailable, the drug design process must rely upon a more indirect approach, the quantitative structure-activity relationships (QSAR) approach [3-23].

In the absence of detailed structural data upon biological receptors, a QSAR model establishes a statistical relationship between the biological activity exerted by a series of compounds and a set of parameters determined from the structures of the compounds [1,2]. The central assumption of a QSAR model is that the numerical value of a specified biological activity measured for a set of molecules depends on the structure of these molecules. In order to correlate with a QSAR model the biological activity and the molecular structure, the structure must be adequately described in a numerical form with a large variety of structural descriptors [1,2]: empirical (Hammett and Taft substituent constants), physical properties (octanol-water partition coefficient, dipole moment, aqueous solubility), constitutional (counts of various molecular subgraphs), topological indices,

* Tables II, III and IV are available in electronic form at: www.edpsciences.org.

geometrical descriptors (molecular surface and volume), quantum (atomic charges, HOMO and LUMO energies), molecular fields (steric, electrostatic, and hydrophobic) [3,6,16,21] or molecular similarity indices [18,19].

Usually, the effect of a drug is a result of its noncovalent interaction with a specific site on a biological target. Frequently, in ligand design one determines the experimental activity for the interaction between a ligand and a biological target without any information on the structure of the active site. Using the experimental activity for a set of compounds that have a high affinity for the active site, one can generate a virtual receptor site that models the ligand-receptor interactions [6,16,17]. A 3D QSAR equation based on a virtual receptor model should give good predictions that can guide the synthesis of new compounds with a good affinity for the investigated receptor. Although a precise definition of 3D QSAR is still lacking, we can identify two components that are essential for this type of models. The first component in the definition of a 3D QSAR model is the computation of the structural descriptors from the three-dimensional molecular structure; various geometrical, quantum, or molecular field descriptors were proposed in recent years. The second component in a 3D QSAR model is an explicit mathematical structure-activity relationship established between a dependent variable (biological activity) and a set of independent variables (3D structural descriptors); the mathematical 3D QSAR equations can be computed with the help of a large number of statistical models, such as multilinear regression, partial least squares (PLS), or neural networks. From the various 3D QSAR models proposed for the construction of a virtual receptor based on the structures and activities of known ligand molecules [1-23], the comparative molecular field analysis (CoMFA) [6,7] model gained a widespread recognition. The CoMFA procedure consists of the following steps: all molecules in the study set are superimposed (aligned); the aligned molecules are placed in a box that is larger in all directions than the volume occupied by the superimposed compounds; the box is partitioned into a grid with points separated usually by 2 Å; various probe atoms are used to compute for each molecule the steric and electrostatic fields in every grid point; the molecular fields are correlated with the biological data by applying the PLS analysis to the field values from the grid points; the CoMFA model is tested for prediction usually with the leave-one-out cross-validation method. In 3D QSAR investigations, the molecular grid contains regions of highly intercorrelated descriptors, and PLS is an efficient algorithm to extract the structural information and correlate it with a biological activity. However, a major drawback of the PLS model is the detrimental influence of structural descriptors that are not correlated with the investigated property; the use of such descriptors adds noise to the model and lowers the statistical quality of the calibration and prediction QSAR equations. An efficient variable selection method, GOLPE (generating optimal linear PLS estimations), was recently proposed [22,23]; this algorithm gives 3D QSAR models with better calibration and prediction results, and significantly reduces the number of structural descriptors used in the computation of the PLS equations. In this way, the time needed to establish a 3D QSAR model is greatly decreased, because only significant variables are considered in calculation.

In the present paper we describe a 3D QSAR procedure that generates a virtual receptor represented as points on a surface (unlike in CoMFA and related algorithms, where the points are places into a 3D box). The comparative receptor surface analysis (CoRSA) is developed in three steps. In the first one, the surface of the virtual receptor is generated using the most active members of a series of compounds. Then, the structural descriptors of the model are determined by computing the total interaction energies between each surface point of the virtual receptor and all atoms in a molecule. In the third step a partial least squares (PLS) data analysis uses the set of structural descriptors to generate a structure-activity model. CoRSA is applied to a set of compounds that act as calcium channel agonists on guinea pig left atrium, giving good calibration and prediction results.

Comparative receptor surface analysis

The development of a comparative receptor surface analysis model consists of the following steps:

(1) The geometry of all molecules in the study set is optimized with molecular mechanics or quantum mechanics methods. Any information regarding the active conformations of the ligands in the actual receptor must be used to optimize the appropriate molecular geometry.

(2) All optimized molecules are aligned (superimposed) using some pharmacophore hypothesis. The CoRSA model depends on the molecules alignment and errors in this step can provide 3D-QSAR models that have a low predictive power. Several alignment assumptions have to be investigated in order to identify the best model.

(3) A subset of the most active molecules is selected to generate the virtual receptor model.

(4) A virtual receptor is generated using information on the geometry, volume, atomic charges, hydrophobicity, hydrogen bonding, or other properties of the aligned molecules. Unlike real receptors, the virtual receptor is not formed by atoms. One or more active molecules are used to generate the three-dimensional receptor surface and to establish the properties of each point on the receptor surface; these compounds form the receptor generation set (RGS) of molecules. The central assumption is the complementarity between the shape and properties of these molecules and the virtual receptor. The three-dimensional receptor surface is represented by points that posses certain properties (charge, hydrophobicity, hydrogen bonding propensity). The coordinates of these points are generated from the shape field of the RGS molecules.

(5) Each surface point from the virtual receptor contains information about the local properties of the receptor. These properties include electrostatic potential, partial charge, hydrophobicity, and hydrogen-bonding propensity. This information is used to compute the interaction energy between the virtual receptor and a molecule. The surface point properties are complementary to those exhibited by the RGS molecules.

(6) With the virtual receptor model defined in steps (1)-(5), the ligand-receptor interaction of a set of molecules is evaluated by computing their interaction energy with the virtual receptor. For a molecule a set of descriptors is formed by computing the interaction energy between each surface point from the virtual receptor and the atoms in the molecule. These descriptors are stored in a QSAR table together with the biological activity of the investigated molecule.

(7) The resulting QSAR table, that can contain several hundred descriptors for each molecule, is used to develop a 3D-QSAR model using the PLS algorithm.

In the present paper the virtual receptor is generated with the receptor surface model proposed by Hahn [16,17], but any other algorithm that generates a receptor model can be used. We present some details of the algorithm that generates the receptor surface.

A steric surface representing the virtual receptor is generated to enclose the set of aligned molecules. The surface of the virtual receptor is generated by a volumetric field (shape field), characterizing molecular shape, which is produced for each aligned molecule. The shape fields from each individual molecule are combined to produce a final volumetric shape field from which an explicit surface is generated. First, a three-dimensional regularly spaced grid is superposed over the aligned set of molecules; the grid box dimensions are extended several Å in each direction from the coordinates of every molecule. The steric field is computed for each point of the grid, and an isosurface of the field is used to generate the surface of the virtual receptor. Two field functions are used to create the shape of the virtual receptor, namely the van der Waals field function and the Wyvill field function. Each field source corresponds to an atom. The van der Waals field function generated by the atom i from a molecule is:

$$V(r_{ij})_i = r_{ij} - r_{\mathrm{VDW},i} \qquad (1)$$

where r_{ij} is the distance from the atom i and the grid point j and $r_{\mathrm{VDW},i}$ is the van der Waals radius of the atom i. This field function, which is computed for every grid point, has the property that inside the van der Waals volume the value is negative, outside the volume the value is positive, and at the van der Waals surface the value $V(r)$ is zero. If a grid point contains a shape field value computed for a different atom, the smaller of the two values is assigned to that grid point. The Wyvill function is a bounded function that decays completely in a finite distance R:

$$V\left(r_{ij}\right)_i = -\frac{4\,r_{ij}^6}{9\,R^6} + \frac{17\,r_{ij}^4}{9\,R^4} - \frac{22\,r_{ij}^2}{9\,R^2} + 1 \qquad (2)$$

where r_{ij} is the distance from the atom i and the grid point j. A field value is the sum of the field values contributed by each atom; if a grid point is outside of R, its shape field value is not computed. The value of R depends on the atom type, and usually its value is twice the van der Waals radius of the atom i. This function has the properties that $V(0) = 1$, $V(R) = 0$, and $V(R/2) = 1/2$. Using the shape field values the marching cubes isosurface algorithm produces a set of triangulated surface points representing the surface of the virtual receptor. The default grid spacing of 0.5 Å yields an average surface density of 6 points/Å^2. This gives an average distance between neighboring points (points in the same triangle) of about 0.47 Å.

After a surface is created, several properties of the virtual receptor associated with each surface point are assigned; these properties include partial charge, electrostatic potential, hydrogen-bonding propensity, and hydrophobicity. These values are used when calculating interaction energy between a molecule and a surface model.

CoRSA model of calcium channel agonist activity

The transmission of electric signals in excitable cells such as nerve or muscle uses voltage-gated ion channels that allow ions to traverse the lipid bilayer surrounding a cell. These ion channels are characterized by a high selectivity, each type of ion channel allowing only one specific ion to traverse it; for example, potassium channels transport only K^+ ions through the membrane. A novel class of calcium channel-modulating compounds, representing alkyl or cycloalkyl 1,4-dihydro-2,6-dimethyl-3-nitro-4-pyridyl-5-pyridinecarboxylates, were recently discovered [24,25]. Their *in vitro* activities as calcium channel modulators were determined with guinea pig ileum longitudinal smooth muscle (GPILSM) and guinea pig left atrium (GPLA). In this series of compounds, the 2-pyridyl isomers act as GPLA agonists and GPILSM antagonists, while the 3-pyridyl and 4-pyridyl isomers act as calcium channel agonists on both GPLA and GPILSM. In this section we present the development of a CoRSA model for the calcium channel GPLA agonists [25].

Data set

The structure and *in vitro* activities of the 13 alkyl or cycloalkyl 1,4-dihydro-2,6-dimethyl-3-nitro-4-pyridyl-5-pyridinecarboxylates is presented in table I. The $\log(1/EC_{50})$ data were used as dependent variables in the PLS model.

Table I. Chemical structures and experimental calcium channel agonist activity, log(1/EC50)exp, of alkyl (or cycloalkyl) 1,4-dihydro-2,6-dimethyl-3-nitro-4-pyridyl-5-pyridinecarboxylates.

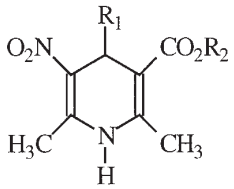

No.	R_1	R_2	$log(1/EC_{50})_{exp}$
1	3-pyridyl	ethyl	5.05
2	4-pyridyl	ethyl	5.19
3	2-pyridyl	$MeOCH_2CH_2$	5.01
4	2-pyridyl	*iso*-butyl	5.04
5	3-pyridyl	*iso*-butyl	5.76
6	4-pyridyl	*iso*-butyl	5.07
7	4-pyridyl	*tert*-butyl	5.55
8	3-pyridyl	cyclopentyl	5.48
9	4-pyridyl	cyclopentyl	5.37
10	2-pyridyl	cyclohexyl	5.43
11	3-pyridyl	cyclohexyl	5.56
12	4-pyridyl	cyclohexyl	5.31
13	2-pyridyl	*iso*-propyl	5.01

Computational and modeling tools

Computer modeling was done using a Silicon Graphics Indigo/R10000 computer running under the IRIX 6.0 operating system. The molecules were constructed using the Cerius[2] 3D-Sketcher and minimized with the CVFF95 force field using the conjugated gradient algorithm. The alignment of the molecules, the computation of the receptor surface model with the Hahn algorithm [16,17], and the PLS analysis were done with the corresponding modules from Cerius[2] [26]. All computations were performed at the Centre de Modélisation et d'Imagerie Moléculaire de l'Université de Nice-Sophia Antipolis (France).

Alignment rule

The most active compound **5** was selected as alignment target, giving good calibration and prediction models. A view of all the aligned compounds **1**-**13** is offered in figure 1.

Virtual receptor generation

The receptor surface model (RSM) proposed by Hahn [16,17] was used to generate the surface of the virtual receptor. A closed receptor model was generated using the van der Waals and the Wyvill field functions, as implemented in RSM.

Surface descriptors computation

Using the virtual receptor, the ligand-receptor interaction energies of the molecules **1**-**13** were evaluated in each and every point of the virtual receptor with the RSM algorithm as implemented in Cerius[2]. For each molecule we have computed the steric, electrostatic, and total interaction energy with every point on the surface of the virtual receptor. Because the presence of a large number of descriptors poorly correlated with the $\log(1/EC_{50})$ of the calcium channel agonists adds noise to the 3D QSAR equation and gives an unstable PLS model, with poor prediction capacity, we have applied in all experiments a simple descriptor selection method. From the entire pool of structural descriptors, we have selected for the PLS analysis a percentage of 3 % of surface points with highest squared correlation coefficient r^2. All descriptors are zero centered and scaled to unit variance.

Partial least squares analyses

The mathematical analyses of the relationships between the ligand-receptor interaction energies and the biological activity were done using the partial least squares algorithm from Cerius[2]. Because the objective of a QSAR study is to derive a model that is optimally predictive, we have estimated the optimal number of components of the PLS model with the leave-one-out cross-validation algorithm.

In table II we present the statistical indices of the CoRSA models obtained in different experiments. The surface of the virtual receptor was generated with all aligned molecules, with the most active 5 compounds (molecules **5**, **6**, **7**, **9** and **10**), and from the most active compound **5** alone. For all these three experiments, the receptor surface was generated either with the van der Waals or Wyvill field functions. Finally, the number of PLS components of the CoRSA model was successively increased, and the leave-one-out cross-validation was used to determine the optimal number

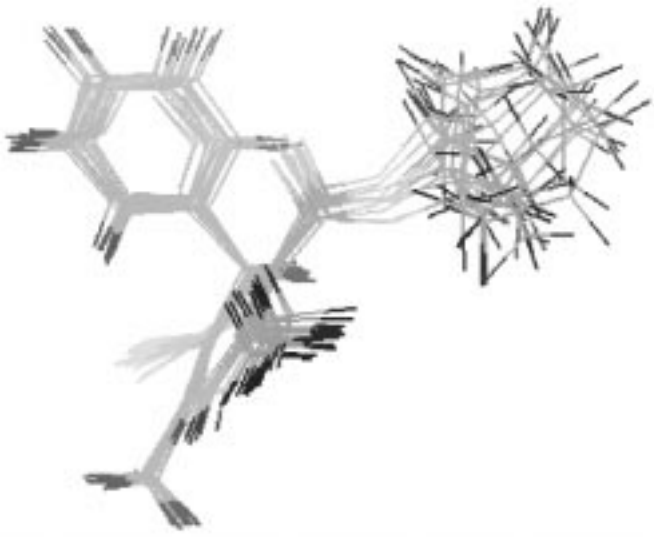

Figure 1. View of all the aligned compounds 1-13.

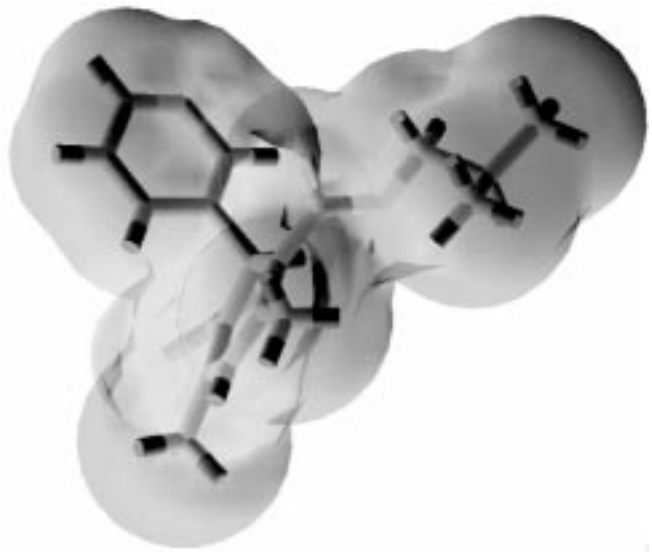

Figure 2. The virtual receptor surface model computed with the van der Waals function. Compound 5 is aligned in the receptor model.

of components. All these results, collected in table II, offer the possibility to select the best combination for the CoRSA model.

In a first test, the van der Waals field function was used to generate the receptor surface from the 13 aligned compounds, using the most active compound **5** as alignment target. The best prediction results are obtained with 5 PLS components, when r^2_{cal} = 0.970 and r^2_{pr} = 0.846; the corresponding calibration and prediction residuals are presented in table III, columns 3 and 4. In a second experiment, the most active 5 compounds generated a van der Waals receptor; the optimum number of PLS is again 5, with r^2_{cal} = 0.987 and r^2_{pr} = 0.926; the calibration and prediction residuals are given in table IV, columns 3 and 4. Although in calibration the difference is not high, in prediction the improvement is considerable. A third experiment considered the van der Waals receptor obtained from the most active compound **5**, that gives r^2_{cal} = 0.992 and r^2_{pr} = 0.960 with 5 PLS components; compared with the previous experiments, a significant improvement of the QSAR model is obtained, as can be seen from the calibration and prediction residuals given in table V, columns 3 and 4. In conclusion, for a receptor surface generated with the van der Waals field function, the best results are obtained when the virtual receptor is complementary to the shape of the compound **5**. In figure 2 we present the virtual receptor surface computed with the van der Waals field function from the shape of compound **5**.

The next set of experiments considered receptor surfaces generated with the Wyvill field function. When the surface was computed with all 13 aligned compounds, the optimum number of PLS components is determined to be 5; the calibration and prediction residuals of this model, with r^2_{cal} = 0.975 and r^2_{pr} = 0.910, are presented in table III, columns 5 and 6. With a Wyvill receptor obtained from the most active 5 molecules (compounds **5**, **6**, **7**, **9** and **10**), the CoRSA model with 3 components gives much worse results, *i.e.* r^2_{cal} = 0.813 and r^2_{pr} = 0.774; the calibration and prediction residuals are given in table IV, columns 5 and 6. Finally, when compound **5** was used to compute the Wyvill receptor, we have obtained a fairly good CoRSA model with 3 components, having r^2_{cal} = 0.903 and r^2_{pr} = 0.849; the corresponding residuals are given in table V, columns 5 and 6. The conclusion obtained from the virtual receptor constructed with a Wyvill field function is that the best CoRSA model is obtained from all molecules in the data set. This result is at variance with the previous result obtained with the van der Waals field function. However, we can explain this divergence by the differences in the two functions, as can be seen by comparing Eqs. (1) and (2): the van der Waals gives a "hard" receptor, very similar with the surface area of the compounds that generate the receptor, while the Wyvill function gives a "soft" receptor, a fuzzy representation of the molecular surface area, with much larger limits.

Conclusion

In this paper we defined a novel 3D-QSAR algorithm of the comparative receptor surface analysis, CoRSA. The model generates a virtual receptor model and computes ligand-receptor energies that can be used as descriptors in a PLS analysis. CoRSA is related to both receptor surface model proposed by Hahn [16,17] and CoMFA proposed by Cramer [6]: the virtual receptor is generated with the RSM algorithm, while the 3D-QSAR models are generated with PLS, like in CoMFA. We have to mention here that the RSM algorithm can be replaced with other methods of computing the surface of a virtual receptor. This approach can be applied for the analysis of data sets whenever the activity information is available but the structure of the receptor site is unknown. The CoRSA model was tested on a set of 13 calcium channel guinea pig left atrium agonists, giving good calibration and prediction results. All the computations were performed with various modules available in Cerius[2].

Acknowledgments

Ovidiu Ivanciuc thanks the Ministère de l'Éducation Nationale, de l'Enseignement Supérieur et de la Recherche of France for a PAST grant. Teodora and Ovidiu Ivanciuc acknowledge the kind hospitality of the LARTIC group during their stay in Nice. We acknowledge the partial financial support of this research by the Romanian Ministry of National Education under Grant 33084 T94.

References

1. Kubinyi, H. *Drug Discovery Today* **1997**, *2*, 457-467.
2. Kubinyi, H. *Drug Discovery Today* **1997**, *2*, 538-546.

3. Rhyu, K.-B.; Patel, H. C.; Hopfinger, A. J. *J. Chem. Inf. Comput. Sci.* **1995**, *35*, 771-778.
4. Klein, C. D. P.; Hopfinger, A. J. *Pharm. Res*. **1998**, *15*, 303-311.
5. Kato, Y.; Itai, A.; Iitaka, Y. *Tetrahedron* **1987**, *43*, 5229-5236.
6. Cramer III, R. D.; Patterson, D. E.; Bunce, J. D. *J. Am. Chem. Soc*. **1988**, *110*, 5959-5967.
7. Clark, M.; Cramer III, R. D.; Jones, D. M.; Patterson, D. E.; Simeroth, P. E. *Tetrahedron Comput. Methodol*. **1990**, *3*, 47-59.
8. Snyder, J. P.; Rao, S. N. *Chem. Design Automation News* **1989**, *4*, 13-15.
9. Snyder, J. P.; Rao, S. N. *Cray Channels* **1990**, *11*, 4-12.
10. Vedani, A.; Zbinden, P.; Snyder, J. P. *J. Receptor Research* **1993**, *13*, 163-177.
11. Vedani, A.; Zbinden, P.; Snyder, J. P.; Greenidge, P. A. *J. Am. Chem. Soc*. **1995**, *117*, 4987-4994.
12. Zbinden, P.; Dobler, M.; Folkers, G.; Vedani, A. *Quant. Struct. Act. Relat*. **1998**, *17*, 122-130.
13. Höltje, H. D.; Anzali, S. *Pharmazie* **1992**, *47*, 691-698.
14. Walters, D. E.; Hinds, R. M. *J. Med. Chem*. **1994**, *37*, 2527-2536.
15. Doweyko, A. M. *J. Med. Chem*. **1994**, *37*, 1769-1778.
16. Hahn, M. *J. Med. Chem*. **1995**, *38*, 2080-2090.
17. Hahn, M.; Rogers, D. *J. Med. Chem*. **1995**, *38*, 2091-2102.
18. So, S.-S.; Karplus, M. *J. Med. Chem*. **1997**, *40*, 4347-4359.
19. So, S.-S.; Karplus, M. *J. Med. Chem*. **1997**, *40*, 4360-4371.
20. Kellogg, G. E.; Semus, S. F.; Abraham, D. J. *J. Comput.-Aided Mol. Design* **1991**, *5*, 545-552.
21. Du, Q.; Arteca, G. A.; Mezey, P. G. *J. Comput. Aided Mol. Design* **1997**, *11*, 503-515.
22. Baroni, M.; Constantino, G.; Cruciani, G.; Riganelli, D.; Valigi, R.; Clementi, S. *Quant. Struct. Act. Relat.* **1993**, *12*, 9-20.
23. Cruciani, G.; Watson, K. A. *J. Med. Chem*. **1994**, *37*, 2589-2601.
24. Vo, D.; Matwoe, W. C.; Ramesh, M.; Iqbal, N.; Wolowyk, M. W.; Howlett, S. E.; Knaus, E. E. *J. Med. Chem*. **1995**, *38*, 2851-2859.
25. Ramesh, M.; Matwoe, W. C.; Akula, M. R.; Vo, D.; Dagnino, L.; Li-Kwong-Ken, M. C.; Wolowyk, M. W.; Knaus, E. E. *J. Med. Chem*. **1998**, *41*, 509-514.
26. Cerius^2, BIOSYM/Molecular Simulations, San Diego, California, USA.

Table II. The optimization of the number of PLS components for the CoRSA models.

PLS Comp.	r^2_{cal}	r^2_{pr}	$PRESS_{pr}$
van der Waals receptor for all molecules			
1	0.507	0.542	0.3450
2	0.768	0.782	0.1642
3	0.887	0.806	0.1460
4	0.933	0.826	0.1313
5	0.970	0.846	0.1160
6	0.985	0.845	0.1165
van der Waals receptor for compounds **5**, **6**, **7**, **9** and **10**			
1	0.576	0.616	0.2894
2	0.804	0.813	0.1405
3	0.882	0.856	0.1085
4	0.953	0.918	0.0619
5	0.987	0.926	0.0559
6	0.997	0.919	0.0609
van der Waals receptor for compound **5**			
1	0.678	0.706	0.2217
2	0.881	0.840	0.1207
3	0.961	0.913	0.0654
4	0.980	0.932	0.0513
5	0.992	0.960	0.0301
6	0.996	0.960	0.0302
7	0.998	0.958	0.0314
Wyvill (soft) receptor for all molecules			
1	0.472	0.504	0.3733
2	0.741	0.760	0.1806
3	0.898	0.869	0.0987
4	0.944	0.890	0.0828
5	0.975	0.910	0.0680
6	0.992	0.893	0.0806
Wyvill (soft) receptor for compounds **5**, **6**, **7**, **9**, and **10**			
1	0.529	0.563	0.3288
2	0.719	0.696	0.2287
3	0.813	0.774	0.1701
4	0.885	0.697	0.2281
Wyvill (soft) receptor for compound **5**			
1	0.542	0.573	0.3217
2	0.812	0.749	0.1893
3	0.903	0.849	0.1137
4	0.926	0.800	0.1503

Table III. Chemical compounds, calcium channel agonist experimental, calibration and prediction residuals for van der Waals and Wyvill (soft) receptors generated with all molecules. Compound 5 was used as alignment target.

N°	$log(1/EC_{50})_{exp}$	*res/cal/W*[a]	*res/pr/W*[b]	*res/cal/S*[c]	*res/pr/S*[d]
1	5.05	–0.02	–0.34	–0.02	–0.25
2	5.19	0.06	0.04	0.07	0.06
3	5.01	–0.01	0.01	–0.02	–0.01
4	5.04	0.03	0.03	0.00	0.00
5	5.76	0.03	0.01	0.04	0.02
6	5.07	–0.02	–0.05	0.00	–0.01
7	5.55	0.00	–0.01	–0.04	–0.04
8	5.48	0.00	–0.02	–0.02	–0.02
9	5.37	0.00	0.03	–0.01	0.00
10	5.43	–0.03	–0.03	–0.03	–0.02
11	5.56	0.07	0.05	0.07	0.05
12	5.31	–0.10	–0.04	–0.05	–0.02
13	5.01	0.00	–0.03	0.02	–0.01

[a] res/cal/W, the calibration residual, $log(1/EC_{50})_{exp} - log(1/EC_{50})_{cal}$, for the closed receptor surface model computed with the van der Waals field function

[b] res/pr/W, the prediction residual, $log(1/EC_{50})_{exp} - log(1/EC_{50})_{pr}$, for the closed receptor surface model computed with the van der Waals field function

[c] res/cal/S, the calibration residual, $log(1/EC_{50})_{exp} - log(1/EC_{50})_{cal}$, for the closed receptor surface model computed with the Wyvill (soft) field function

[d] res/pr/S, the prediction residual, $log(1/EC_{50})_{exp} - log(1/EC_{50})_{pr}$, for the closed receptor surface model computed with the Wyvill (soft) field function

Table IV. Chemical compounds, calcium channel agonist calibration and prediction residuals for van der Waals and Wyvill (soft) receptors generated with compounds 5, 6, 7, 9, and 10. Compound 5 was used as alignment target. The notations are explained in table III.

N°	$log(1/EC_{50})_{exp}$	*res/cal/W*	*res/pr/W*	*res/cal/S*	*res/pr/S*
1	5.05	0.00	–0.22	–0.13	–0.34
2	5.19	0.03	0.01	0.07	0.04
3	5.01	–0.02	–0.03	0.04	0.02
4	5.04	0.05	0.04	–0.17	–0.15
5	5.76	0.00	–0.01	0.11	0.01
6	5.07	–0.03	0.00	–0.07	–0.03
7	5.55	0.03	0.04	0.04	0.01
8	5.48	–0.03	–0.04	–0.04	–0.01
9	5.37	–0.01	0.00	–0.13	–0.09
10	5.43	–0.02	–0.02	–0.02	0.01
11	5.56	0.04	0.04	0.21	0.17
12	5.31	–0.04	–0.04	–0.01	–0.03
13	5.01	–0.01	–0.02	0.09	0.05

Table V. Chemical compounds, calcium channel agonist calibration and prediction residuals for van der Waals and Wyvill (soft) receptors generated with compound 5. The notations are explained in table III.

Nº	*log(1/EC$_{50}$)$_{exp}$*	*res/cal/W*	*res/pr/W*	*res/cal/S*	*res/pr/S*
1	5.05	0.00	–0.17	–0.10	–0.28
2	5.19	0.01	–0.01	0.09	0.02
3	5.01	–0.01	–0.01	0.03	0.05
4	5.04	–0.02	0.00	–0.10	–0.10
5	5.76	–0.01	0.00	0.08	0.03
6	5.07	0.02	0.01	–0.04	–0.07
7	5.55	–0.01	0.00	0.01	0.03
8	5.48	–0.03	–0.02	0.11	0.05
9	5.37	0.02	0.01	–0.04	–0.06
10	5.43	0.00	–0.01	–0.06	–0.01
11	5.56	0.05	0.04	0.04	0.07
12	5.31	–0.02	–0.02	–0.10	–0.09
13	5.01	0.01	0.01	0.09	0.08